

# TSFool: Crafting High-quality Adversarial Time Series through Multi-objective Optimization to Fool Recurrent Neural Network Classifiers

Yanyun Wang<sup>1,2</sup> Dehui Du<sup>1</sup> Yuanhao Liu<sup>1</sup>

<sup>1</sup>*Software Engineering Institute, East China Normal University*

Shanghai, China

dhdu@sei.ecnu.edu.cn

<sup>2</sup>*Department of Computer Science, The University of Hong Kong*

Hong Kong, China

ynwang@connect.hku.hk

**Abstract**—Deep neural network (DNN) classifiers are vulnerable to adversarial attacks. Although the existing gradient-based attacks have achieved good performance in feed-forward model and image recognition tasks, the extension for time series classification in the recurrent neural network (RNN) remains a dilemma, because the cyclical structure of RNN prevents direct model differentiation and the visual sensitivity to perturbations of time series data challenges the traditional local optimization objective to minimize perturbation. In this paper, an efficient and widely applicable approach called TSFool for crafting high-quality adversarial time series for the RNN classifier is proposed. We propose a novel global optimization objective named Camouflage Coefficient to consider how well the adversarial samples hide in class clusters, and accordingly redefine the high-quality adversarial attack as a multi-objective optimization problem. We also propose a new idea to use intervalized weighted finite automata (IWFA) to capture deeply embedded vulnerable samples having otherness between features and latent manifold to guide the approximation to the optimization solution. Experiments on 22 UCR datasets are conducted to confirm that TSFool is a widely effective, efficient and high-quality approach with 93.22% less local perturbation, 32.33% better global camouflage, and 1.12 times speedup to existing methods.

**Index Terms**—adversarial attack, time series classification, recurrent neural network

## I. INTRODUCTION

Advanced DNN classifiers can automatically extract key features from datasets and generate accurate predictions. As a widely accepted explanation for this effectiveness, the *manifold hypothesis* states that DNN classifiers distinguish different classes by latent manifold hyperplane [1]. However, research has shown that DNN classifiers are vulnerable to adversarial attacks [2], which means imperceptible perturbations in the input can cause significant changes in the output [3]. A rich body of adversarial attack works have been proposed to cope with this dilemma by discovering and interpreting the defects of DNN classifiers and generating adversarial samples to enhance the robustness of the models. For instance, the common methods based on model gradient [4], [5], [6] have achieved good performance in the context of feed-forward DNN classifiers and image recognition tasks.

However, those gradient-based adversarial attacks always assume that the target model is directly differentiable, while the unique time recurrent structure of RNN prevents this computation [7]. On the other hand, as time series are far more visually sensitive to perturbations than image data, on such data the feasibility and fairness of the current local optimization objective followed by existing attacks to minimize the perturbation amount for every single sample are doubtful since it looks like to be tailored for image data. As a consequence, while time series classification is encountered in various real-world safety-critical tasks ranging from health care to food safety [8] and RNN is one of the most effective structures that the state-of-the-art models in such field relying on [9], the existing methods do not work well to generate adversarial time series for RNN classifiers. Currently, some efforts have been made to deal with this problem, yet the idea to make RNN differentiable by cyclical computational graph unfolding [7] is not efficient and scalable enough in practice, and the black-box attacks for time series like [8] rely on the adversarial transferability to avoid RNN only get very limited success.

In this paper, we propose an efficient and widely applicable approach named TSFool to craft high-quality adversarial time series for RNN classifiers. With an argument that the imperceptibility of adversarial samples defined under the current local optimization objective is flawed and does not always lead to high-quality attacks, we propose a novel global optimization objective named Camouflage Coefficient to take the relative position between adversarial samples and class clusters into consideration to measure how well the adversarial samples hide without being noticed, and add it as another objective to make the adversarial attack a multi-objective optimization problem. To practically and efficiently approximate the solution, we locate the misclassified samples deeply embedded in a positive cluster as the indicator, and accordingly pick fragile samples as attack targets and guide them across a near hyperplane on a position close to the indicator. We propose a new idea to introduce a representation model that can simulate the manifold hyperplane of a classifier but distinguish inputs

by visual features like human to capture the indicator that has otherness between latent manifold and external features. As a targeted design for RNN, the weighted finite automaton (WFA) is intervalized as the representation model.

Our evaluation on 22 UCR time series datasets and LSTM classifiers demonstrate that TSFool works well widely, achieving the average number of generated time series 1117, adversarial rate of 39.05% and a decrease of model accuracy of 0.1275. In the comparison with FGSM and DeepFool, the TSFool achieves at least 93.22% less average local perturbation, 32.33% less average global Camouflage Coefficient and 1.12 times average speedup. And the great advantages in the comparison with the black-box BIM attack also confirm the necessity of the target design for RNN.

## II. BACKGROUND AND RELATED WORK

### A. Adversarial Attack Basics

The concept of adversarial attack is firstly introduced in [2], where an adversarial sample  $\vec{x}^*$  crafted from a legitimate sample  $\vec{x}$  is defined by an optimization problem:

$$\vec{x}^* = \vec{x} + \delta_{\vec{x}} = \vec{x} + \min \|\vec{z}\| \text{ s.t. } f(\vec{x} + \vec{z}) \neq f(\vec{x}) \quad (1)$$

where  $f : \mathbb{R}^n \rightarrow \vec{y}$  is the targeted ML classifier and  $\delta_{\vec{x}}$  is the smallest perturbation according to a norm appropriate for the input domain. Since exactly solving this problem by an optimization method is time-consuming [6] and not always possible, especially in DNNs with complex non-convexity and non-linearity [7], the common practice is to find the approximative solutions to estimate adversarial examples.

The two most famous attack approaches namely the *fast gradient sign method* (FGSM) [4] and the *forward derivative method* [5] are both gradient-based, which means the perturbation is guided by the differentiating functions defined over the architecture and parameters of the targeted classifier. To be specific, FGSM implements a perturbation according to the gradient of the cost function  $\mathcal{L}$  with respect to the input  $\vec{x}$ :

$$\delta_{\vec{x}} = \varepsilon \text{ sign}(\nabla_{\vec{x}} \mathcal{L}(f, \vec{x}, \vec{y})) \quad (2)$$

where  $\varepsilon$  denotes the magnitude of the perturbation, while to quantified evaluate how a specific input component  $x_i$  modifies the output component  $f_j$ , the forward derivative is defined as the Jacobian of the classifier:

$$J_f[i, j] = \frac{\partial f_j}{\partial x_i} \quad (3)$$

The following work DeepFool [6] further introduces the classification hyperplane and determines the perturbation direction of a specific sample by its nearest hyperplane to implement the attack greedily, and the *basic iterative method* (BIM) [10] extends FGSM by applying it iteratively with a small step size and clip the obtained samples after each step, both of which are proposed for smaller perturbations.

### B. Dilemma of Adversarial Attack in RNN and Time Series

While the existing approaches work well on feed-forward DNNs and (mainly) image data, this success has not carried over to RNN time series classification. There are two main reasons for the dilemma. For one thing, the presence of cyclical computations in the architecture of RNN prevents direct model differentiation based on the chain rule [7], which presents challenges to the applicability of all the gradient-based approaches. For another, unlike the image data in which the imperceptibility to human eyes is respectively easier to achieve in practice, time series data are so visually sensitive to perturbations that there is a stricter requirement for it [9].

An intuitive solution for the first problem mentioned is to make the model differentiable by cyclical computational graph unfolding to fit the gradient-based approaches [7]. However, as the length of time series is usually long in the real world, the efficiency and scalability of the unfolded computation are of concern in practice. And although the number of time steps perturbed is firstly proposed as a norm to measure the quality of adversarial time series in [7], the quantitative analysis of perturbation amplitude which is even more important is still absent. Another idea is to craft adversarial time series using an acyclic model like Residual Network (ResNet) [8], and then rely on the adversarial transferability to implement a black-box attack. Unfortunately, although such attacks do realize micro perturbation and avoid the hassle of targeted designing for the RNN, a later experiment will show that it may only get limited success in practice. All in all, the dilemma caused by the recurrent structure of RNN and perturbation sensitivity of time series remains to be considered further.

## III. MOTIVATION

### A. Manifold Hypothesis in Adversarial Problem

The *manifold hypothesis* is one of the widely accepted explanations for the effectiveness of DNNs. It holds that many high-dimensional datasets in the real world are actually distributed along low-dimensional manifolds embedded in high-dimensional space [11], which explains why DNNs can find potential key features as complex functions of a large number of features in the data and generate accurate predictions. It is through learning the latent manifold of the training data that DNNs can realize manifold interpolation between input samples, so as to correctly process and predict unseen samples [1]. As a result, what matters in DNN classification is how to distinguish the latent manifolds of samples from different classes instead of the original features. However, due to the limitation of sampling technologies and human cognitive ability, practical label construction and model evaluation usually have to rely on a specific form of data with external features in the high-dimensional space.

Thus, one of the possible explanations for the existence of the adversarial sample is that, the features of the input data cannot always fully and visually reflect the latent manifold, which makes it possible for samples that are considered to be similar in the external features to have radically different latent

manifolds, and as a result, to be understood and processed in a different way by the DNN. Therefore, even a small perturbation in human cognition imposed on the correct sample may completely overturn the DNN's view of its latent manifold, so as to result in a completely different result.

### B. High-quality Adversarial Sample

The sensitivity of time series data forces us to rethink the hidden dangers in the perturbation control in existing methods. Firstly, common methods always implement perturbations to all of the training samples, while there must be individuals among them that are easier or harder to be perturbed respectively depending on the specific distribution. Without taking this difference into account and picking target samples appropriately, it is almost impossible for the perturbation amount to be stably controlled by the attack approaches themselves, but it has to depend heavily on the datasets. Secondly, we argue that the approximation of the optimal perturbation in (1) does not always lead to a high-quality adversarial attack in practice, while all the common approaches view it as the ultimate goal and accordingly define the relative perturbation ratio  $\rho$  as the quality metric of the adversarial sample  $\vec{x}^*$ :

$$\rho(\vec{x}^*) = \frac{\|\delta_{\vec{x}}\|}{\|\vec{x}\|} \quad (4)$$

The problem is when we jump out of the single sample and consider it from the perspective of classes, it can be found that the smallest perturbation is not necessarily the most imperceptible. For instance, as shown in Fig. 1, the adversarial sample  $x_1$  is crafted from  $x_0$  through a minimal perturbation estimated just as the DeepFool, while it is obvious that another adversarial sample  $x_2$  is more at risk of being mistaken as the original class. And actually, these cases are relatively rare but indeed appear in all of our experiments.

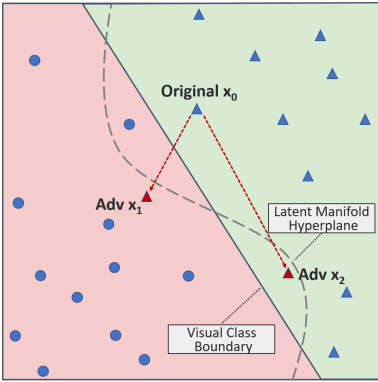


Fig. 1. An instance that the smallest perturbation is not necessarily the most imperceptible in the global perspective.

This inspired us to define the high-quality adversarial sample from a global view. Given that  $\mathcal{X}_i$  is the set of samples with label  $i$  in the training set under a  $k$ -class classification task. For  $\vec{x} \in \mathcal{X}_i$ , the **Camouflage Coefficient**  $\mathcal{C}$  of the corresponding adversarial sample  $\vec{x}^*$  is defined as:

$$\mathcal{C}(\vec{x}^*) = \frac{\|\vec{x}^* - \vec{m}_{ori}\|/d_{ori}}{\|\vec{x}^* - \vec{m}_{adv}\|/d_{adv}} \quad (5)$$

where the centre of mass of the  $i$ -th class is shaped in the form of a legitimate sample  $m_i = \frac{1}{|\mathcal{X}_i|} \sum_{x_j \in \mathcal{X}_i} x_j$ , and the average distance between the centre of mass and all the samples in the  $i$ -th class is calculated as  $d_i = \frac{1}{|\mathcal{X}_i|} \sum_{x_j \in \mathcal{X}_i} \|x_j - m_i\|$  to eliminate the potential unfairness from the difference in the distribution range of different classes. Just as the saying goes, "the best place to hide a leaf is in the woods". The Camouflage Coefficient represents the relative proportion of the norm distance between the adversarial sample and the original class to the distance between it and the misclassified class regarding the different cluster ranges of the classes, so it can tell us to what extent an adversarial example can blend into the original class without being noticed. The smaller the value, the higher the quality of the adversarial sample. While if the value exceeds 1, we can say the camouflage is a relative failure because that means the misclassification of the adversarial sample is no longer surprising as it already looks more like the samples belong to that class. In our approach, we introduce the Camouflage Coefficient as another optimization target along with (1), and also add it as an evaluation metric for the high-quality adversarial sample.

### C. Adversarial Attack through Multi-objective Optimization

After taking the Camouflage Coefficient into consideration, the adversarial attack becomes a multi-objective optimization problem. Just as the common approaches, we do not solve it directly considering the practice efficiency, but find the approximative solution in a logical and pragmatic way. Obviously, the best choice to optimize (5) itself is to make  $\vec{x}^*$  closer to the  $\vec{m}_{ori}$ , which also means farther away from the  $\vec{m}_{adv}$  most of the time. On the other hand, exceeding the nearest manifold hyperplane is proven a successful method in DeepFool to approximate the optimization objective in (1). So as a compromise to account for both of them at the same time, a natural idea is to cross a hyperplane that is relatively near the target sample  $\vec{x}$  on a place that is relatively close to the  $\vec{m}_{ori}$ .

To make this idea practical, we can find a misclassified sample  $\vec{x}_s$  deeply embedded in a target class as the indicator, and then accordingly pick the correctly classified sample that is the nearest to  $\vec{x}_s$  in that class as the target  $\vec{x}$ . In this way, when we modify  $\vec{x}$  in the direction of  $\vec{x}_s$  to approximate the manifold hyperplane between them, we can not only acquire a considerable value of Camouflage Coefficient because the embedded  $\vec{x}_s$  itself is a sample closer to  $\vec{m}_{ori}$  than to  $\vec{m}_{adv}$ , but also expect the hyperplane is relatively close to  $\vec{x}$  rely on the fact that it is closest to  $\vec{x}_s$  among its class. In fact, from our experiment results, we believe that in most cases the hyperplane selected in our approach is the nearest one, the same as DeepFool, while we hardly approach it along the shortest distance. The perturbation crafted as above can be denoted as fellow:

$$\delta_{\vec{x}} = \lambda_{\varepsilon} \|\vec{x}_s - \vec{x}\| + \vec{x}_{\varepsilon} \quad (6)$$

where  $\lambda_{\varepsilon} \|\vec{x}_s - \vec{x}\|$  is the maximum modification that makes  $\vec{x}$  approach  $\vec{x}_s$  under a given granularity  $\varepsilon$  without changing

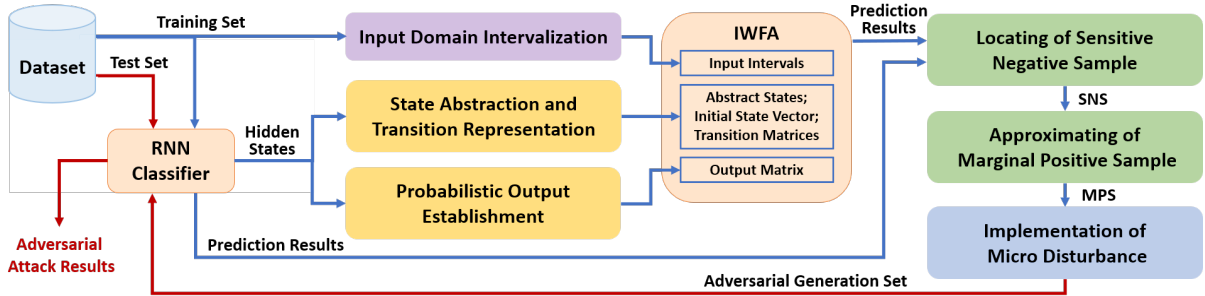


Fig. 2. The Roadmap of TSFool.

its original predicted class, and  $\vec{x}_\varepsilon$  is a micro stochastic disturbance under the same  $\varepsilon$  added for crossing the hyperplane.

Now the only problem left is how to find the  $\vec{x}_s$ , so it is time to recall the foreshadowing in III-A. According to the analysis, if there is a kind of representation model that can simulate the way a classifier understands and processes input data, but distinguish different inputs by their original features in the high-dimensional space just like a human, then it can be used to capture the otherness between the latent manifold and external features of any input sample. And such otherness can serve as the guidance to find the  $\vec{x}_s$  since it is essentially a potentially vulnerable sample that visually and actually belongs to one class but is misclassified to another class because of the wrong latent manifold of the target classifier. The novel adversarial attack approach proposed in this paper is just based on all the above motivations.

#### IV. APPROACH

By realizing the above idea in the field of RNN time series classification, we propose our novel approach named TSFool with the roadmap shown in Fig. 2. In this section, we provide a detailed description of the TSFool, including the establishment of a representation model of the RNN classifier, the locating of  $\vec{x}_s$ , and the crafting of adversarial time series.

##### A. Establishment of Intervalized Weighted Finite Automaton

One of the most important elements in the cyclical computation of RNN is the hidden state updated every time step. So to take all the recurrent information into consideration and well simulate the process of execution and prediction of the RNN classifier, we introduce WFA [12] and improve it to be intervalized so that it can serve as the representation model in our idea better. An **Intervalized Weighted Finite Automaton (IWFA)** from a  $y$ -class RNN classifier  $\mathcal{N}$  is defined as a tuple  $\mathcal{A} = (Z, S, \mathcal{I}, (E_\zeta)_{\zeta \in Z}, \mathcal{T})$ , where  $Z$  is a finite set of intervals that cover the whole input domain,  $S$  is a finite set of states abstracted from  $\mathcal{N}$ ,  $\mathcal{I}$  is the initial state vector of dimension  $|S|$ , and  $\mathcal{T}$  is the probabilistic output matrix with size  $|S| \times y$ ; For any interval  $\zeta \in Z$ , the corresponding probabilistic transition matrix of all the samples fall into the interval is  $E_\zeta$  with size  $|S| \times |S|$ . The  $\mathcal{I}$  will be constantly updated as the carrier of state changes in RNN execution and reproduces state transformations under different inputs at each

time step with the corresponding  $E_\zeta$ , followed by the  $\mathcal{T}$  to simulate the computation of probabilistic classification results.

Due to the limited space, we give the full process of IWFA establishment as Alg. 1 with a description of the intervalization only, and recommend [12] for more details. The WFA introduces existing clustering methods like  $k$ -means in the input dataset, and uses all the instance features in any single cluster to build the corresponding probabilistic transition matrix, to simulate the generalization of the RNN classifier. Nevertheless, to force IWFA to distinguish different inputs strictly by external features as a human and to make the shape and the granularity of the partition more reasonable and controllable, which also benefits the perturbation in IV-B3, we change from the data clustering to the domain intervalization. To be specific, for every single time series, we calculate the average  $L_2$  distance between its features of every pair of adjacent time steps respectively for each of the feature dimensions, and then reduce them by an order of magnitude as a ‘‘micro distance’’. The reason is that when the size of the input interval is less than the corresponding ‘‘micro distance’’ in all the feature dimensions respectively in every single time step, it is almost impossible for instance features that actually belong to different clusters to be assigned to the same input interval, so as to ensure the effectiveness of the input domain intervalization.

We provide an instance of IWFA execution for intuitive understanding. For a two-classification task, given an input time series  $X$  with three time steps and the input  $x_i$  of each time step falls into the input intervals  $\zeta_i$ :

$$X = [x_1, x_2, x_3]_{(x_i \in \zeta_i)}, S = [s_0, s_1, s_2], \mathcal{I} = [1 \ 0 \ 0],$$

$$E_{\zeta_1} = \begin{bmatrix} 1/4 & 0 & 3/4 \\ 0 & 0 & 0 \\ 0 & 0 & 0 \end{bmatrix}, E_{\zeta_2} = \begin{bmatrix} 1/4 & 1/4 & 1/2 \\ 1 & 0 & 0 \\ 1/2 & 1/2 & 0 \end{bmatrix},$$

$$E_{\zeta_3} = \begin{bmatrix} 0 & 1 & 0 \\ 0 & 1/4 & 3/4 \\ 1/4 & 1/2 & 1/4 \end{bmatrix}, \text{ and } \mathcal{T} = \begin{bmatrix} 1/2 & 1/2 \\ 0 & 1 \\ 3/4 & 1/4 \end{bmatrix},$$

the execution process can be illustrated as:

$$\mathcal{I} \cdot \left( \prod_{i=1}^{|X|} E_{\zeta_i} \right) \cdot \mathcal{T} = \mathcal{I} \cdot E_{\zeta_1} \cdot E_{\zeta_2} \cdot E_{\zeta_3} \cdot \mathcal{T}$$

$$\begin{aligned}
&= [1 \ 0 \ 0] \cdot \begin{bmatrix} 1/4 & 0 & 3/4 \\ 0 & 0 & 0 \\ 0 & 0 & 0 \end{bmatrix} \cdot E_{\zeta_2} \cdot E_{\zeta_3} \cdot \mathcal{T} \\
&= [1/4 \ 0 \ 3/4] \cdot \begin{bmatrix} 1/4 & 1/4 & 1/2 \\ 1 & 0 & 0 \\ 1/2 & 1/2 & 0 \end{bmatrix} \cdot E_{\zeta_3} \cdot \mathcal{T} \\
&= [7/16 \ 7/16 \ 1/8] \cdot \begin{bmatrix} 0 & 1 & 0 \\ 0 & 1/4 & 3/4 \\ 1/4 & 1/2 & 1/4 \end{bmatrix} \cdot \mathcal{T} \\
&= [1/32 \ 39/64 \ 23/64] \cdot \begin{bmatrix} 1/2 & 1/2 \\ 0 & 1 \\ 3/4 & 1/4 \end{bmatrix} \\
&= [73/256 \ 183/256],
\end{aligned}$$

where each of the first operators is a vector with the same size of  $\mathcal{I}$  and elements summing to 1, which represents the “current state” of IWFA updated in the process. The final result is probabilistic just like classifier. In Fig. 3 we further illustrate this execution process in the form of a visualized automaton.

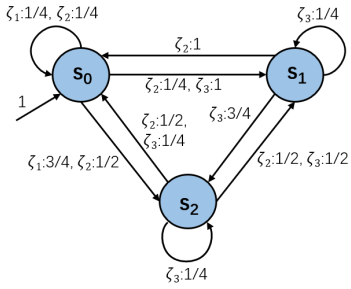


Fig. 3. The visualization of the instance IWFA mentioned.

### B. Crafting High-quality Adversarial Time Series

1) *Locating of Sensitive Negative Sample*: As mentioned in III, after getting the IWFA, we use it as a representation model of the RNN classifier and make a comparison of prediction results between them to capture the otherness between the features and latent manifold in the training data. To be specific, when the prediction of IWFA is correct while that of the RNN classifier is wrong, it means that compared with other samples that are similar in external features and have the same classification category in fact, this sample is processed and understood by RNN as a different latent manifold, so as to be predicted mistakenly. Samples like this are defined as the **Sensitive Negative Sample (SNS)**. There are two important implications that make SNS a useful instance of  $\vec{x}_s$ . For one thing, both the space of features and latent manifold are not discrete but continuous, which means a new sample generated close to the SNS is highly likely to have the same property in this regard. For another, it is obvious that an SNS itself meets the requirements of a high-quality adversarial sample provided that it is not included in the training set. In Alg. 2, we get the prediction results in the training set respectively by using the RNN classifier and the IWFA (lines

---

### Algorithm 1 Establishment of IWFA

---

**Input:** RNN  $\mathcal{N} = (X, Y, H, f, g)$ , Training Dataset  $\mathcal{X}$ , Hyper-parameters  $k, t$  and  $r_{input}$   
**Output:** IWFA  $\mathcal{A} = (Z, S, \mathcal{I}, (E_\zeta)_{\zeta \in Z}, \mathcal{T})$

- 1: Initialize  $Z \leftarrow \emptyset, S' \leftarrow \emptyset, S \leftarrow \emptyset, E \leftarrow \emptyset, \mathcal{T} \leftarrow \emptyset$
- 2:  $t_{input} \leftarrow CalculateTinput(\mathcal{X}, r_{input})$
- 3:  $\mathcal{X}' \leftarrow FeaturesNormalization(\mathcal{X})$
- 4: **while**  $X' \in \mathcal{X}'$  **do**
- 5:   **while**  $x' \in X'$  **do**
- 6:      $\zeta \leftarrow Floor(x') \times t_{input}$
- 7:      $Z.add(\zeta)$
- 8:   **end while**
- 9: **end while**
- 10: **while**  $X \in \mathcal{X}$  **do**
- 11:    $S'' \leftarrow [g(f^{(i)}(X))]_{i=0}^{|X|}$
- 12:    $S'.extend(S'')$
- 13: **end while**
- 14: **while**  $s' \in S'$  **do**
- 15:    $s_{pred} \leftarrow ArgSort(-s')[: k]$
- 16:    $s_{conf} \leftarrow Floor((-Sort(-s')[: k]) \times t)$
- 17:    $s \leftarrow Concat(s_{pred}, s_{conf})$
- 18:    $S.add(s)$
- 19: **end while**
- 20:  $\mathcal{I} \leftarrow Zeros(|S| + 1)$
- 21:  $\mathcal{I}[0] \leftarrow 1$
- 22: **while**  $\zeta \in Z$  **do**
- 23:    $E_\zeta \leftarrow RecordingTransition^{x' \in \zeta}(\mathcal{X}')$
- 24:   **while**  $E_\zeta[i] \in E_\zeta$  **do**
- 25:     **if**  $Sum(E_\zeta[i]) \neq 0$  **then**
- 26:        $E_\zeta[i] \leftarrow E_\zeta[i]/Sum(E_\zeta[i])$
- 27:     **end if**
- 28:   **end while**
- 29:    $E.append(E_\zeta)$
- 30: **end while**
- 31: **while**  $s \in S$  **do**
- 32:    $\mathcal{T}_s \leftarrow RecordingPrediction^{s' \in s}(S')$
- 33:    $\mathcal{T}_s \leftarrow \mathcal{T}_s/Sum(\mathcal{T}_s)$
- 34:    $\mathcal{T}.append(\mathcal{T}_s)$
- 35: **end while**
- 36: **return**  $\mathcal{A} = (Z, S, \mathcal{I}, (E_\zeta)_{\zeta \in Z}, \mathcal{T})$

---

4-5), followed by a comparison between them in the function *FindSensitiveNegSample* to find the SNS (line 6).

2) *Approximating of Marginal Positive Sample*: Different from the common practices that implement adversarial attacks in each of the samples in the training set, our approach picks out specific target samples according to the SNS. The **Targeted Positive Sample (TPS)** is defined as a sample that is closest to a specific SNS in the interval distance among the whole training set and gets a correct prediction that is the same as the supervised label of the SNS from the classifier. So given that an SNS and its corresponding TPS are similar in external features and have the same supervised label, while they are predicted differently by the classifier, between them there must

be a hyperplane between the latent manifold of the two classes respectively having the label as the supervised label and the incorrect prediction of SNS. Accordingly, we define the **Marginal Positive Sample (MPS)** as a sample approximating that hyperplane generated by the feature interpolation of a pair of SNS and TPS (i.e.  $\vec{x} + \lambda_\epsilon \|\vec{x}_s - \vec{x}\|$ ), and predicted to be the same class as TPS. Since the feature interpolation makes sure that it does not deviate from the range of the positive class visually and the approximating to the hyperplane makes it vulnerable to perturbations, the MPS can serve as a parent sample for adversarial attack aiming at the corresponding TPS.

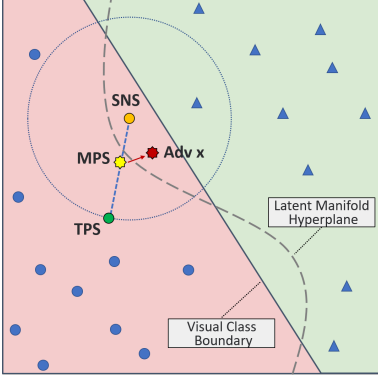


Fig. 4. An intuitive illustration for crafting high-quality adversarial samples.

As shown in Alg. 2, we find the TPS for each of the SNS by the function *FindTargetedPosSample* (lines 7-8), and then with the hyper-parameter  $g$  indicates the granularity for the average sampling in the given range (lines 10-11) and the function *UpdateSampRange* determines the new sampling range for the next turn according to the two adjacent samples generated this turn with different prediction results respectively as the SNS and TPS (lines 12-13), we recursively approximate the MPS until the granularity of the sampling step is less than the set perturbation amplitude (lines 14-15). It should be noted that, since there is the otherness between features and latent manifold, the samples generated by feature interpolation from SNS to TPS may repeatedly cross the latent manifold hyperplane of the two considered classes many times, which means the optional range for the sampling may be more than one in some specific turns. In that case, we stipulate that the range closest to the TPS is always selected because the closer the finally acquired MPS is to the TPS, the higher the quality of the adversarial samples generated subsequently since MPS is their parent.

3) *Implementation of Micro Perturbation*: When we get an MPS by sampling at a specific granularity, a child sample of it generated under perturbation  $\vec{x}_\epsilon$  with the same granularity can easily cross the latent manifold hyperplane, so as to become an adversarial sample of the corresponding TPS. In other words, the property of adversarial of the generated samples are guaranteed by their parent MPS, so the only thing to consider in the perturbation is that it must be micro enough to make sure that the children can inherit the visual consistency between

---

**Algorithm 2** Crafting High-quality Adversarial Time Series

---

**Input:** RNN  $\mathcal{N} = (X, Y, H, f, g)$ , IWFA  $\mathcal{A} = (Z, S, \mathcal{I}, (E_\zeta)_{\zeta \in Z}, \mathcal{T})$ , Training Dataset  $\mathcal{X}$ , Training Labels  $\mathcal{Y}$ , Hyper-parameters  $g$ ,  $f_{ampl}$  and  $f_{win}$

**Output:** Adversarial Time Series Set  $\mathcal{X}_{adv}$

```

1: Initialize  $\mathcal{X}_{adv} \leftarrow []$ 
2:  $p_{ampl} \leftarrow CalculatePerturbationAmplitude(f_{ampl})$ 
3:  $p_{win} \leftarrow CalculatePerturbationWindowSize(f_{win})$ 
4:  $Y_{rnn} \leftarrow \mathcal{N}(\mathcal{X})$ 
5:  $Y_{iwfa} \leftarrow \mathcal{A}(\mathcal{X})$ 
6:  $X_{sns} \leftarrow FindSensitiveNegSample(\mathcal{X}, \mathcal{Y}, Y_{rnn}, Y_{iwfa})$ 

7: while  $x_{neg} \in X_{sns}$  do
8:    $x_{pos} \leftarrow FindTargetedPosSample(\mathcal{X}, x_{neg})$ 
9:   while  $x_{mps}$  not exist do
10:     $x_{step} \leftarrow (x_{pos} - x_{neg})/g$ 
11:     $X_{samp} \leftarrow Sampling(x_{neg}, x_{pos}, x_{step})$ 
12:     $Y_{samp} \leftarrow \mathcal{N}(X_{samp})$ 
13:     $x_{neg}, x_{pos} \leftarrow UpdateSampRange(X_{samp}, Y_{samp})$ 
14:    if  $x_{step} < p_{ampl}$  then
15:       $x_{mps} \leftarrow x_{pos}$ 
16:    end if
17:   end while
18:    $X_{adv} \leftarrow MicroPerturbation(x_{mps}, p_{ampl}, p_{win})$ 
19:    $\mathcal{X}_{adv}.append(X_{adv})$ 
20: end while
21: return  $\mathcal{X}_{adv}$ 

```

---

the MPS and the TPS to guarantee the quality of them. To ensure the micro perturbation, the perturbation amplitude is determined under the limitation of the “micro distance” mentioned in IV-A, and the size of the perturbation window is constrained to be an order of magnitude lower than the number of time step of the time series input, with the hyper-parameters  $f_{ampl}$  and  $f_{win}$  used to allow further adjusting within the limitations in practice (lines 2-3). And finally, through sliding the window time step by time step and applying random perturbations to the MPS under the above setting by the function *MicroPerturbation*, a series of adversarial time series are generated and recorded (lines 18-19).

## V. EVALUATION AND DISCUSSION

In this section, we will verify the effectiveness and advantages in efficiency and attack quality of TSFool in three series of experiments. The Long Short-Term Memory (LSTM) is adopted to establish the RNN classifiers, and the publicly available UCR time-series archive [13] provides 22 datasets for the experiments. We choose them following the UCR briefing document to make sure there is no cherry-picking. The code and the detailed records including the pre-trained models, the raw experiment data and the crafted adversarial sets are available on the Github repository: <https://github.com/FlaAI/TSFool-adversarial-time-series-generation-to-fool-RNNs>

TABLE I

THE TABLE SHOWS THE EXPERIMENT RECORDS IN THE 22 UCR DATASETS WITH TSFOOL, INCLUDING THE ORIGINAL ACCURACY OF CLASSIFIERS, THE SIMILARITY BETWEEN CLASSIFIER AND IWFA, THE SIZE AND ADVERSARIAL RATE OF GENERATION SET, AND THE ATTACK EFFECTS IN TEST SET.

Dataset	Training Accuracy	IWFA Similarity	Generation Number	Adversarial Rate	Test Accuracy	
					Original	Attacked
CBF	0.7667	93.33%	234	<b>37.61%</b>	0.7511	<b>0.7249</b>
DPOAG	0.8525	76.00%	2926	<b>32.02%</b>	0.7842	<b>0.6845</b>
DPOC	0.7767	70.50%	2920	<b>41.92%</b>	0.7319	<b>0.5904</b>
DPTW	0.8150	76.00%	146	<b>28.08%</b>	0.7122	<b>0.6842</b>
ECG2	0.8800	74.00%	704	<b>46.59%</b>	0.7900	<b>0.5659</b>
ECG5	0.9480	92.60%	254	<b>46.85%</b>	0.9267	<b>0.9056</b>
GP	0.9400	88.00%	272	<b>25.37%</b>	0.9333	<b>0.8033</b>
IPD	0.9701	77.61%	48	<b>47.92%</b>	0.9650	<b>0.9424</b>
MPOAG	0.7875	88.50%	1314	<b>47.34%</b>	0.6429	<b>0.5272</b>
MPOC	0.7017	95.33%	584	<b>49.32%</b>	0.7457	<b>0.5863</b>
MPTW	0.6767	56.89%	146	<b>35.62%</b>	0.6169	<b>0.6033</b>
PPOAG	0.8200	79.25%	2336	<b>29.97%</b>	0.8976	<b>0.7131</b>
PPOC	0.7800	76.00%	8322	<b>33.38%</b>	0.7869	<b>0.6677</b>
PPTW	0.7775	94.00%	1314	<b>35.39%</b>	0.8000	<b>0.6570</b>
SC	0.9400	78.67%	330	<b>49.70%</b>	0.9400	<b>0.7111</b>
TP	0.9990	69.40%	234	<b>41.03%</b>	0.9993	<b>0.9766</b>
GPAS	0.8000	88.89%	544	<b>40.62%</b>	0.8418	<b>0.6349</b>
GPVMF	0.9630	79.26%	816	<b>49.88%</b>	0.9652	<b>0.6307</b>
GPOVY	0.9926	95.59%	272	<b>38.97%</b>	0.9778	<b>0.7445</b>
PC	0.9500	82.78%	524	<b>20.42%</b>	0.9444	<b>0.8281</b>
SS	0.9267	84.00%	60	<b>43.33%</b>	0.9133	<b>0.7905</b>
UMD	0.8056	77.78%	272	<b>37.87%</b>	0.7847	<b>0.6731</b>

Firstly, we show the great effectiveness of TSFool by applying it in all of the 22 datasets in Table. I. By carefully designing the value of the hyper-parameters, we keep the accuracy of the classifiers in the training and test set respectively from 0.6767 to 0.9990 and from 0.6169 to 0.9993, and make the IWFA similarity values range from 56.89% to 95.59%, which is calculated by comparing the prediction results of every single input time series between the classifier and IWFA. As a result, we can say that the 22 experiments have covered most of the situations that might be seen in practice regarding the quality of the different classifiers and the IWFAAs established accordingly, so the experiment results are of general significance. To be specific, TSFool works well in all the experiments. The average number of crafted time series is 1117, and the average rate that a time series in an adversarial generation set is indeed an adversarial sample is 39.05%. We then implement adversarial attacks to the original classifiers by a merger between the corresponding adversarial generation set and test set. All the attacks successfully make the test accuracy of the classifier drop, with the average decrease of 0.1275 from 0.8387 to 0.7112. The results confirm that the TSFool is highly effective and generally applicable in the adversarial attack of the RNN time series classifier.

Secondly, we show the considerable advantages of TSFool in the attack efficiency and the quality of crafted time series by the comparisons with FGSM and DeepFool mentioned in II-A. We implement the comparisons in three datasets namely the GPMVF, GPOVY and PC, on which TSFool respectively

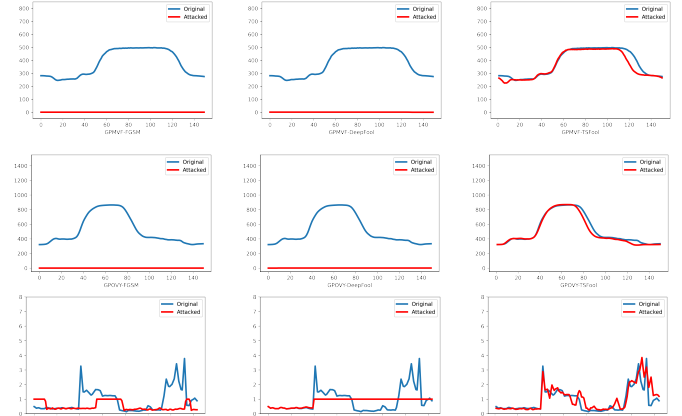


Fig. 5. Corresponding to Table. II, the figures show the instances of adversarial time series generated by FGSM, DeepFool and TSFool in the three representative datasets. The FGSM and DeepFool actually fail to get any useful information to guide the perturbation to the GPMVF and GPOVY, while they work in the PC (also with not satisfying results yet). This instability is just caused by recurrent structures that prevent gradient computing. In contrast, with a targeted design for RNN, TSFool works well in all the datasets.

achieves the adversarial rate that is the maximum (49.88%), the closest to the average value (38.97%) and the minimum (20.42%) among the total 22 experiments above, to ensure the results are fair and of general significance. As shown in Table. II, the number of time series generated in a single

TABLE II

THE TABLE SHOWS THE ADVERSARIAL ATTACK RESULTS OF FGSM, DEEPFOOL AND TSFOOL IN THE THREE REPRESENTATIVE DATASETS, INCLUDING THE AVERAGE VALUE OF TIME COST (S), RELATIVE PERTURBATION RATIO AND CAMOUFLAGE COEFFICIENT FOR CRAFTING A SINGLE TIME SERIES.

Dataset	Approach	Generation Number	Adversarial Rate	Test Accuracy		Average Time Cost	Average Perturbation	Camouflage Coefficient
				Original	Attacked			
GPMVF	FGSM	135	52.59%	0.9652	0.8182	0.012274	50.77%	0.4932
	DeepFool	135	55.56%		0.8093	3.988831	49.69%	0.5035
	<b>TSFool</b>	<b>816</b>	<b>49.88%</b>		<b>0.6307</b>	<b>0.008148</b>	<b>1.19%</b>	<b>1.1340</b>
GPOVY	FGSM	136	47.79%	0.9778	0.7583	0.010798	49.53%	2.3647
	DeepFool	136	47.79%		0.7583	4.957071	44.35%	2.0197
	<b>TSFool</b>	<b>272</b>	<b>38.97%</b>		<b>0.7445</b>	<b>0.009951</b>	<b>1.88%</b>	<b>0.4201</b>
PC	FGSM	180	50.00%	0.9444	0.7111	0.005413	6.27%	1.9886
	DeepFool	180	54.44%		0.6889	3.832390	8.70%	1.6071
	<b>TSFool</b>	<b>524</b>	<b>20.42%</b>		<b>0.8281</b>	<b>0.006654</b>	<b>3.80%</b>	<b>0.9344</b>

execution of TSFool is significantly larger than that of the other two approaches. For the average time cost to craft every single time series, the weighted means on the three datasets show that TSFool (0.007967s) is slightly better than FGSM (0.009091s) and dramatically better than DeepFool (4.218368s). It seems that FGSM and DeepFool have advantages in adversarial rate and are also comparable to TSFool in the attack effect. However, it makes no sense to talk about this in isolation without considering the sample quality. In fact, it can be found that no matter under the traditional metric (4) or under the newly proposed Camouflage Coefficient (5), the quality of adversarial time series crafted by TSFool is much better than that of FGSM and DeepFool. The only exception is the Camouflage Coefficient in GPMVF, because in that 2-class dataset the samples of one class distribute in two divided clusters and the cluster of another class just lies between them. This possibility of misdirection is one of the reasons why we do not use Camouflage Coefficient in the optimization alone.

TABLE III

THE RESULTS OF THE BLACK-BOX ATTACK TRANSFERRED FROM [8] AND THE WHITE-BOX ATTACK BY TSFOOL ON THE IPD DATASET.

Approach	Adversarial Rate	Attacked Test Acc	Average Perturbation	Camouflage Coefficient
BIM*	6.80%	0.9485	2.21%	1.0261
<b>TSFool</b>	<b>47.92%</b>	<b>0.9424</b>	<b>3.11%</b>	<b>0.5453</b>

Finally, as mentioned in II-B, the black-box attacks depend on the transferability of the adversarial sample has achieved good performance. So it is not surprising if there is someone who wonders whether our targeted design for RNN is really necessary given that adversarial time series can be easier generated from other acyclic models. To dispel this doubt, we refer to a mature work [8] that provides adversarial samples for UCR datasets by using the BIM attack in ResNet, and selected the IPD dataset to make a comparison since the work does not cover any of the three representative datasets in Table. II and the attack on IPD is believed to be challenging in [8] because it contains the shortest time series in UCR archive, so as to require a higher perturbation amount. As the comparison results in Table. III, although the adversarial set from [8]

contains as many as 1029 generated time series, its adversarial rate is poor in the RNN classifier, resulting in an inferior attack effect than TSFool with only 48 crafted samples. In this case, its advantage in relative perturbation ratio is also suspicious as most samples considered are actually not adversarial, not to mention the gap in Camouflage Coefficient values. The results verify that adversarial time series generated in an acyclic model can not always effectively attack the RNN classifier for the same task, so as to confirm the necessity of our work.

## VI. CONCLUSION AND FUTURE WORK

In this paper, we propose an efficient and widely applicable adversarial attack method TSFool to craft high-quality adversarial time series for the RNN classifier. The main contributions of this paper are: firstly, we propose a novel global optimization objective named Camouflage Coefficient and redefine the high-quality adversarial attack as a multi-objective optimization problem, which may be instructive to the refining of the adversarial attack theory; secondly, for the first time, we proposed an idea to introduce representation model to capture potentially vulnerable samples having otherness between features and latent manifold to reduce the candidate target samples to improve the efficiency and quality of adversarial attack, which can also be easily transferred to other types of models and data, so as to provide a new feasible way for the community to craft adversarial samples. For future works, deeply exploring the newly defined multi-objective optimization problem to find better approximative solutions is an interesting topic, and the attempts to further realize our idea in other kinds of adversarial attacks are in progress at present.

## ACKNOWLEDGMENT

This work is an extension of Yanyun Wang's Bachelor's Degree Thesis and was mainly done when he was an undergraduate student at the Software Engineering Institute, East China Normal University under the supervision of Prof. Dehui Du and in cooperation with a master's student Yuanhao Liu. Yanyun Wang is currently a master's student in the Department of Computer Science, The University of Hong Kong.

## REFERENCES

- [1] F. Chollet, *Deep learning with Python*. Simon and Schuster, 2021.
- [2] C. Szegedy, W. Zaremba, I. Sutskever, J. Bruna, D. Erhan, I. Goodfellow, and R. Fergus, “Intriguing properties of neural networks,” *arXiv preprint arXiv:1312.6199*, 2013.
- [3] X. Huang, D. Kroening, W. Ruan, J. Sharp, Y. Sun, E. Thamo, M. Wu, and X. Yi, “A survey of safety and trustworthiness of deep neural networks: Verification, testing, adversarial attack and defence, and interpretability,” *Computer Science Review*, vol. 37, p. 100270, 2020.
- [4] I. J. Goodfellow, J. Shlens, and C. Szegedy, “Explaining and harnessing adversarial examples,” *arXiv preprint arXiv:1412.6572*, 2014.
- [5] N. Papernot, P. McDaniel, S. Jha, M. Fredrikson, Z. B. Celik, and A. Swami, “The limitations of deep learning in adversarial settings,” in *2016 IEEE European symposium on security and privacy (EuroS&P)*. IEEE, 2016, pp. 372–387.
- [6] S.-M. Moosavi-Dezfooli, A. Fawzi, and P. Frossard, “Deepfool: a simple and accurate method to fool deep neural networks,” in *Proceedings of the IEEE conference on computer vision and pattern recognition*, 2016, pp. 2574–2582.
- [7] N. Papernot, P. McDaniel, A. Swami, and R. Harang, “Crafting adversarial input sequences for recurrent neural networks,” in *MILCOM 2016-2016 IEEE Military Communications Conference*. IEEE, 2016, pp. 49–54.
- [8] H. I. Fawaz, G. Forestier, J. Weber, L. Idoumghar, and P.-A. Muller, “Adversarial attacks on deep neural networks for time series classification,” in *2019 International Joint Conference on Neural Networks (IJCNN)*. IEEE, 2019, pp. 1–8.
- [9] T. Wu, X. Wang, S. Qiao, X. Xian, Y. Liu, and L. Zhang, “Small perturbations are enough: Adversarial attacks on time series prediction,” *Information Sciences*, vol. 587, pp. 794–812, 2022.
- [10] A. Kurakin, I. J. Goodfellow, and S. Bengio, “Adversarial examples in the physical world,” in *Artificial intelligence safety and security*. Chapman and Hall/CRC, 2018, pp. 99–112.
- [11] C. Fefferman, S. Mitter, and H. Narayanam, “Testing the manifold hypothesis,” *Journal of the American Mathematical Society*, vol. 29, no. 4, pp. 983–1049, 2016.
- [12] X. Zhang, X. Du, X. Xie, L. Ma, Y. Liu, and M. Sun, “Decision-guided weighted automata extraction from recurrent neural networks,” in *Thirty-Fifth AAAI Conference on Artificial Intelligence (AAAI)*. AAAI Press, 2021, pp. 11 699–11 707.
- [13] H. A. Dau, A. Bagnall, K. Kamgar, C.-C. M. Yeh, Y. Zhu, S. Gharghabi, C. A. Ratanamahatana, and E. Keogh, “The ucr time series archive,” *IEEE/CAA Journal of Automatica Sinica*, vol. 6, no. 6, pp. 1293–1305, 2019.